
**Separation Science and Technology**
Publication details, including instructions for authors and subscription information:
http://www.informaworld.com/smpp/title~content=t713708471

# Membrane Partition and Mass Transfer in Ultrafiltration

Héléne De Balmann[a]; Pierre Aimar[a]; Victor Sanchez[a]
[a] LABORATOIRE DE GENIE CHIMIQUE - CNRS UNIVERSITÉ PAUL SABATIER, TOULOUSE CEDEX, FRANCE

**To cite this Article** De Balmann, Héléne , Aimar, Pierre and Sanchez, Victor(1990) 'Membrane Partition and Mass Transfer in Ultrafiltration', Separation Science and Technology, 25: 5, 507 — 534
**To link to this Article: DOI:** 10.1080/01496399008050347
**URL:** http://dx.doi.org/10.1080/01496399008050347

SEPARATION SCIENCE AND TECHNOLOGY, 25(5), pp. 507-534, 1990

# Membrane Partition and Mass Transfer in Ultrafiltration

HÉLÈNE DE BALMANN, PIERRE AIMAR, and
VICTOR SANCHEZ

LABORATOIRE DE GENIE CHIMIQUE – CNRS
UNIVERSITÉ PAUL SABATIER
31062 TOULOUSE CEDEX, FRANCE



**Abstract**

Through ultrafiltration experiments with a macromolecular solution of dextran and a suspension of bentonite, it is shown how the understanding of mass transfer phenomena involved in ultrafiltration can be improved if several limiting mechanisms working simultaneously over different parts of a same membrane are taken into account. This partition is determined according to the operating conditions as well as the characteristics of the treated fluid. This approach is convenient to describe an entire range of experimental variations in solvent and solute transfer through hollow fiber membranes induced either by macromolecular concentration polarization or by particles fouling. It is shown that reversible fouling can have effects as dramatic as irreversible fouling (pore plugging) in some circumstances.

## INTRODUCTION

The performances of ultrafiltration systems depend on several parameters, among them the nature of the membrane, the fluid characteristics, and the operating conditions (hydrodynamic, temperature, pressure, duration). They can be evaluated using the permeate flux, $J$, and the rejection coefficient, $T.R.$, defined for a solute by the relationship

$$T.R. = 1 - (C_p/C_0) \tag{1}$$

Many studies have been dedicated to variations in the permeate flux with the operating conditions and to provide some models describing the observed results.

In ultrafiltration of macromolecular solutions, it has been shown that in the absence of any physicochemical interaction between the solutes and the membrane material, the transfer of solvent is controlled by concentration polarization due to a build-up near the membrane of the retained molecules (*1*, *2*). Various models exist, but one of the most commonly used assumes that the concentration gradient existing between the two sides of the membrane induces an osmotic pressure that partially balances the applied pressure (*2*). On the other hand, few models are available for the ultrafiltration of suspensions. The cake filtration model (*3–5*) is often used although it is more adapted to traditional filtration. It assumes that each particle carried to the membrane surface by the filtration of the solvent accumulates there to form a static deposit, called a "cake." According to this mechanism, the filtration rate should continuously decrease with time. Such a prediction disagrees with most of the experimental results obtained in the ultrafiltration of suspensions, for they show that the permeate flux reaches a stationary value. Other models have therefore been proposed to account for the existence of this steady state. The scour model (*6*) assumes that some particles led to the membrane surface by solvent filtration are removed because of a scouring effect due to the tangential flow of the feed solution. Hence, it becomes possible to explain the existence of the stationary thickness of the cake, i.e., a stationary value of the permeate flux versus time, and to explain its dependence on the operating parameters. Another approach has recently been proposed (*7*) to account for the forces involved on a microscopic scale. According to this analysis, which assumes the particles to be independent of each other, the motion of a particle depends on the relative importance of two forces generated by the filtration of the solvent through the pores of the membrane and by the tangential flow of the feed. The ratio of these two forces determines whether or not a particle in the feed stream will be deposited on the membrane surface.

Concerning the solute transfer, it has been shown that the rejection coefficient depends on the running parameters, on the membrane and fluid characteristics, and that it could be significantly changed by adsorption of macromolecules (*8–10*) or by fouling due to suspended particles (*11*). On the other hand, some results obtained when these fouling phenomena were eliminated during ultrafiltration of synthetic polymeric

solutions allowed the sole influence of the concentration polarization on the transfer of solutes through the membrane to be studied (*12–15*). It was demonstrated in the latter case that variations in the overall rejection coefficient versus the operating conditions depend on deformation of polymer coils due to the shear stress created by the permeate flow through the pores and on the increase in concentration near the porous wall (*14*, *16*). In addition, the use of gel permation chromatography to analyze the feed and the permeate emphasizes the existence of segregation with respect to the molecular weight in a polydisperse polymeric solution (*16–18*). As a result, the phenomena that act on both the permeate flux and the rejection coefficient also change the molecular weight distribution of the permeate solution. Consequently, only a few models have been proposed to describe variations of solute transport through ultrafiltration membranes (such as the "double-layer model"), in analogy to solute transport in reverse osmosis (*19*, *20*). Since most membranes are asymmetric, porous media are created by the superposition of two parts: the transport of solute through the first one (the dense skin layer) is due to diffusion, while through the second one (the porous support) it is due only to convection. As soon as there is a concentration gradient between the two sides of the membrane, this model predicts the existence of solute transport. This model is not very convenient since for some operating conditions a complete rejection of the solutes is observed in ultrafiltration. A "pore partition model" (*21*) has recently been proposed to describe solute transport through ultrafiltration membranes. This model considers the membrane to have pore size distribution divided into two regions defined according to a given solute size: a complete retentive part, made of the smallest pores through which only the solvent can flow, and a nonselective part, made of the largest pores through which the flow of solvent carries solute molecules.

In the present work we investigate the importance of accounting for pore size distribution in data interpretation for both the ultrafiltration of solutions and of suspensions.

One part of the work is based on a study of the ultrafiltration of a macromolecular dextran solution, and a solute transport model is proposed. This model accounts for the influence of concentration polarization due to the dissolved matter contained in the feed. Another part is based on the ultrafiltration of a clay suspension. Again, a fouling mechanism is proposed to describe the change induced in the membrane by the presence of suspended matter in the processed fluid.

## MATERIAL AND METHODS

### Fluids and Analytical Equipment

The solvent was distilled water containing 1 mg/L $NaN_3$ to prevent bacterial contamination. Two kinds of fluids were used: macromolecular solutions (dextran T70, with an average molecular weight of 70,000 daltons) and bentonite clay suspensions (average diameter, 1.6 μm; minimum size, 0.22 μm). The dextran solutions were prepared by dissolving dried macromolecules in the solvent, while the clay suspensions were prepared by dilution from a concentrated suspension (16 g/kg). The solute concentrations were determined by refractive index measurements (Beckman 156). The suspended solids concentrations were determined by turbidimetry (Hach ratio 2000).



### Ultrafiltration Apparatus and Procedure

All ultrafiltration experiments were carried out at 20°C by using the equipment described by Fig. 1. The concentration of the feed was main-

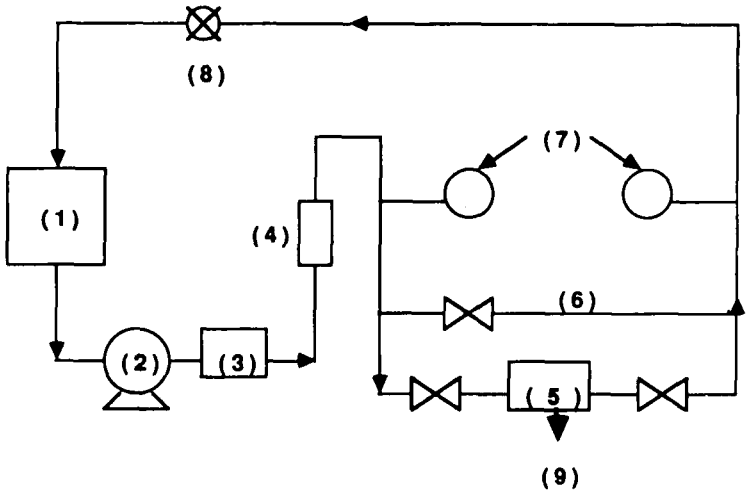


FIG. 1. Ultrafiltration equipment. (1) Feed tank, (2) recirculating pump, (3) thermostat, (4) flowmeter, (5) ultrafiltration module, (6) by-pass, (7) pressure gauges, (8) pressure control valves, (9) balance.

tained constant by recirculating the permeate. The cross flow velocity and the pressure were independently set by using a valve located at the end of the loop. Two pressure gauges are located near the entrance and the outlet of the ultrafiltration module. The average transmembrane pressure, $\Delta P$, is calculated as follows:

$$\Delta P = (P_{\text{inlet}} + P_{\text{outlet}})/2 \tag{2}$$

For given operating conditions, the solvent flux, $J$, and the solute flux, $JC_p$, are recorded versus time. Whatever the operating parameters, the mass transfer reaches a steady state. All the results presented have been measured at steady state.

The permeability of the membranes was measured before and after each run without cleaning. No difference was observed, suggesting that there was no irreversible fouling during ultrafiltration under our conditions.



## Membranes-Modules

Two types of polysulfone hollow fibers were used: 1) outerskinned hollow fibers manufactured according to French Patent IRCHA-CNRS 8,409,225, with an external diameter of 0.37 mm. The module was made of a bundle of 40 fibers sealed in a Plexiglas tubular shell, the diameter and the length of which were 16 and 250 mm, respectively. The active length of the fibers, which were plugged at one end, was 220 mm. The total exchange area was $A = 0.010$ m$^2$. Since the fiber section is negligible, the Reynolds number was calculated by taking the internal diameter of the tubular shell as equivalent to the hydraulic diameter.

The hydraulic permeability of the membrane, measured at 20°C with the solvent, is

$$L_p = 1.2 \times 10^{-7} \text{ kg} \cdot \text{m}^{-2} \cdot \text{s}^{-1} \cdot \text{Pa}^{-1}$$

2) Innerskinned hollow fibers of 0.98 mm internal diameter were supplied by "Lyonnaise des Eaux" (Toulouse, France). Each module was made of a bundle of 50 fibers sealed in a 250-mm long Plexiglas tubular shell. The active length of the fibers was 220 mm, and the total exchange area was $A = 0.034$ m$^2$.

Three membranes of different permeabilities were used:

$$\text{Membrane M1: } L_p = 5.7 \times 10^{-7} \text{ kg} \cdot \text{m}^{-2} \cdot \text{s}^{-1} \cdot \text{Pa}^{-1}$$

Membrane M2: $L_p = 4.3 \times 10^{-7}\ \text{kg} \cdot \text{m}^{-2} \cdot \text{s}^{-1} \cdot \text{Pa}^{-1}$

Membrane M3: $L_p = 3.0 \times 10^{-7}\ \text{kg} \cdot \text{m}^{-2} \cdot \text{s}^{-1} \cdot \text{Pa}^{-1}$

## RESULTS

Figures 2 and 3 show, respectively, the influence of the feed flow rate and the feed concentration on the permeate flux and on the solute mass transfer obtained with the outerskinned hollow fiber membrane and a Dextran T70 solution.

They show that whatever the operating conditions, the shapes of the curves giving the variations of mass transfer versus applied pressure remain the same. Beyond a given pressure value, which depends on the membrane permeability and the operating conditions, any increase in pressure does not change the flux. Such a limiting flux has been reported in many other studies (*1*, *2*). For a characteristic value of transmembrane pressure, the solute mass transfer goes through a maximum. In every case this characteristic pressure is very close to that giving the limiting flux. It therefore seemed convenient to divide the pressure range into two regions separated by a threshold value that depends on both the operating conditions and the membrane properties, and where the predominent mass transfer phenomena would be different. For pressures below this threshold, increasing the applied pressure leads to an increase in the permeate flux as well as in the solute mass transfer, while for pressures above this threshold, increasing the applied pressure has no consequences for the permeate flux but leads to a decrease in the solute transfer.

Figures 4 to 6 show the influence of feed flow rate, feed concentration, transmembrane pressure, and membrane permeability on the permeate flux obtained with innerskinned hollow fiber membranes and a bentonite clay suspension. Whatever the operating conditions, the turbidity of the permeate is nearly zero, indicating that ultrafiltration eliminates even the smallest particles (0.22 μm) contained in the feed. Figure 4 shows that the permeate flux decreases for a few minutes and reaches a steady state. This stationary value depends on the operating conditions and on the membrane properties. In addition, there is a transmembrane pressure value (again depending on the membrane and the operating conditions) beyond which any increase in the applied pressure has no effect on the stationary value of the permeate flux (Fig. 5). This behavior is the same as that observed with macromolecular solutions but is rather unusual in the filtration of suspensions. Another important point is that this limiting flux is fairly independent of membrane permeability (Fig. 6). However, contrary to the

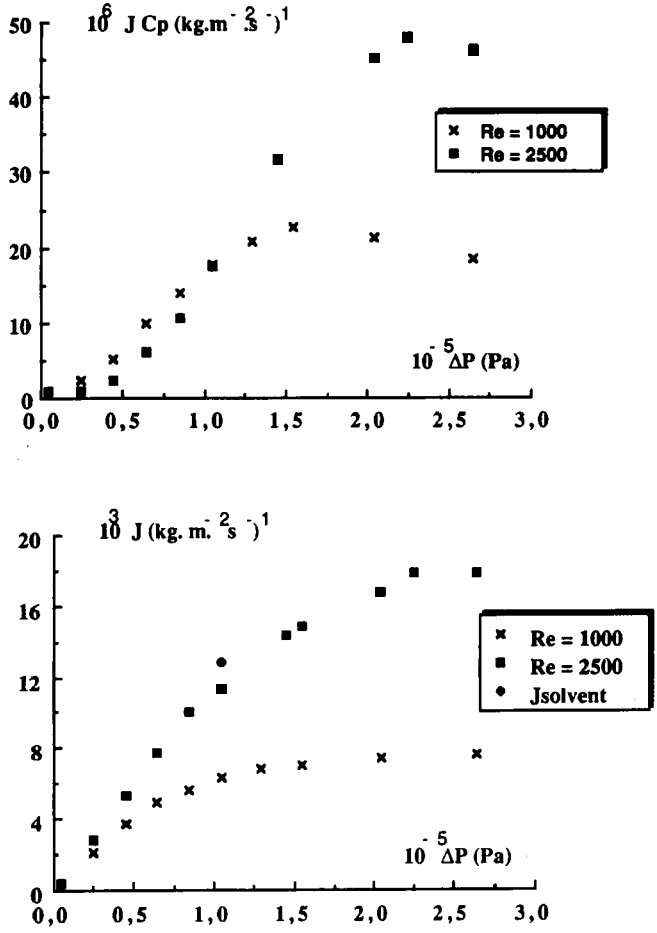


FIG. 2. Ultrafiltration of a dextran solution. Influence of feed flow rate on solvent and solute transfer. Outerskinned hollow fiber membrane. $C_0$ = 10 g/kg.

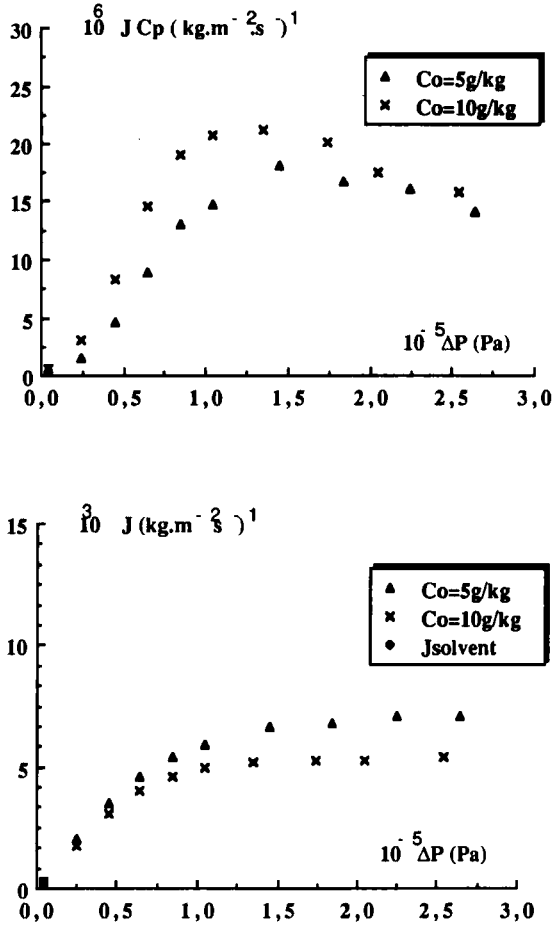


FIG. 3. Ultrafiltration of a dextran solution. Influence of concentration on solvent and solute transfer. Outerskinned hollow fibers. Re = 500.

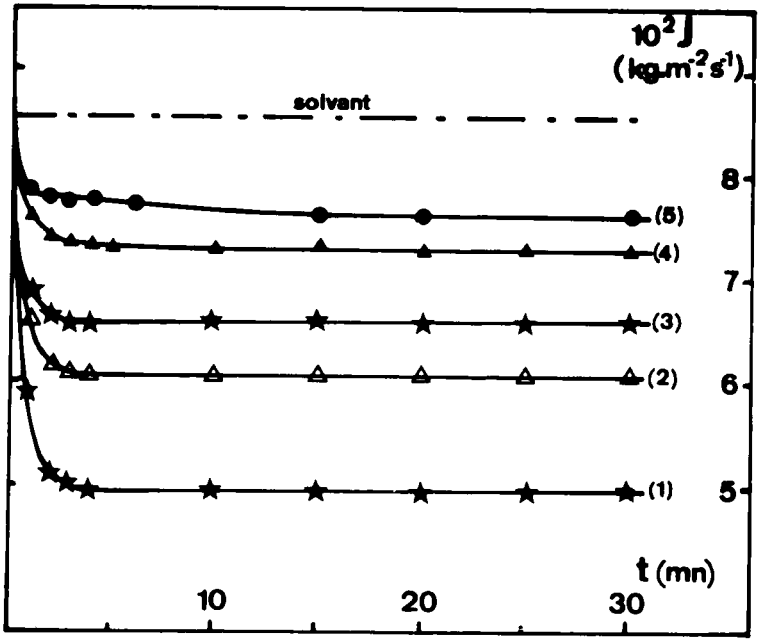


FIG. 4. Ultrafiltration of a clay suspension. Influence of feed flow rate on the permeate flux. Membrane M1. $C_s$ = 1 g/kg, $\Delta P = 1.5 \times 10^5$Pa. (1) $u$ = 0.6 m/s, (2) $u$ = 0.8 m/s, (3) $u$ = 1.1 m/s, (4) $u$ = 1.4 m/s, (5) $u$ = 1.6 m/s.



results obtained during the ultrafiltration of macromolecular solutions, there are some operating ranges, e.g., low pressure, in which the presence of particles does not alter the flux, i.e., the flux is the same as that obtained with pure solvent under the same conditions.

## DISCUSSION

### Solute Transfer Model

Consider the pore partition model (*21*). This model assumes the membrane is divided in two regions defined according to a given size solute: one (Part B) has the smallest pores that retain the solute, the other one (Part A) has the largest pores through which permeation of the solvent

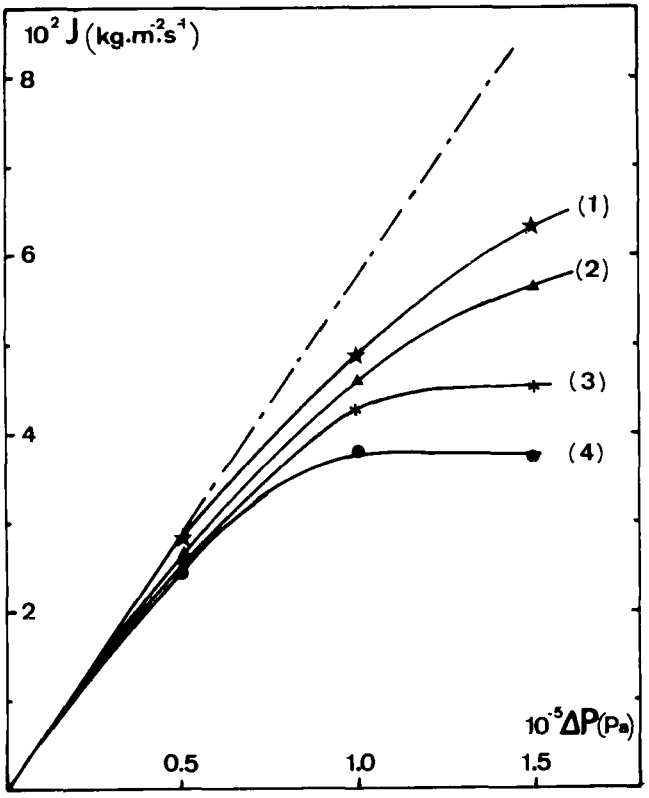


FIG. 5. Ultrafiltration of a clay suspension. Influence of transmembrane pressure and feed concentration on the permeate flux. Membrane M1. $u$ = 0.75 m/s. (1) $C_s$ = 0.5 g/kg, (2) $C_s$ = 1 g/kg, (3) $C_s$ = 2.0 g/kg, (4) $C_s$ = 3.0 g/kg.

carries the solute macromolecules. Consequently, two separate mass transport equations can be written:

$$J = J_A + J_B \tag{3}$$

$$J_s = JC_p = J_AC \tag{4}$$

where $C$ is the concentration of the solution flowing through the pores that allow filtration of the solute. Assuming that polarization is negligible through the nonselective part of the membrane, the permeate flux can be expressed by a filtration law:

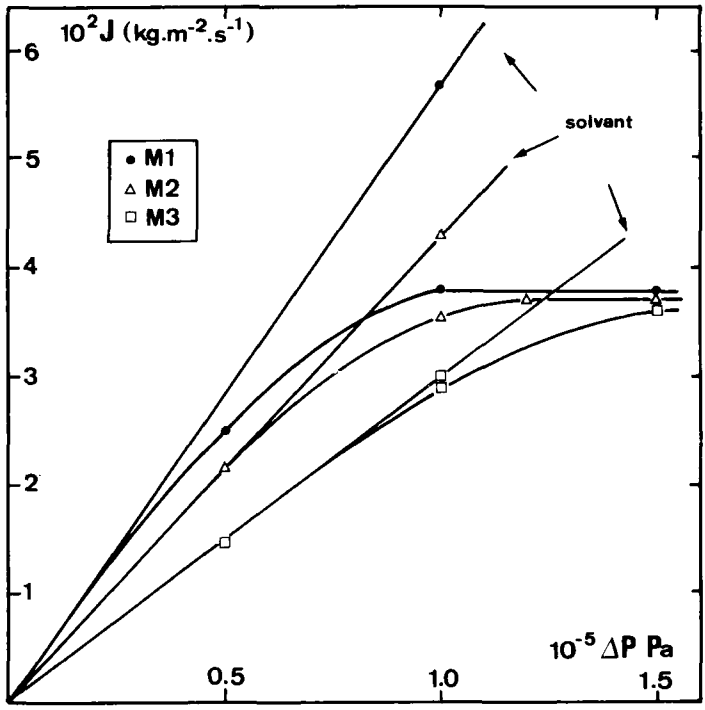


FIG. 6. Ultrafiltration of a clay suspension. Influence of membrane permeability on the variations of permeate flux versus applied pressure. $C_s$ = 3.0 g/kg, $u$ = 0.75 m/s.

$$J_A = \alpha \Delta P / \mu(C) R_h \tag{5}$$

where $\alpha$ represents the fraction of pores that allow the passage of the solute: it is called the "partition parameter" in this paper. On the other hand, the osmotic assumption (2) can be used to express the flux of permeate flowing through the retentive part of the membrane (Part B):

$$J_B = (1 - \alpha)(\Delta P - \Delta \Pi')/\mu_s R_h \tag{6}$$

where $\mu_s$ is the viscosity of the solvent. In these equations, $R_h$ is the hydraulic resistance of the membrane and is constant in our conditions because no irreversible fouling was observed. Combining Eqs. (4) and (5), a solute transfer equation is obtained:

$$JC_p = (\alpha \Delta P/\mu(C)R_h)C \tag{7}$$

These equations involve membrane characteristics ($R_h$), physicochemical properties of the solution ($\mu$, $\Pi$), as well as some parameters that depend on both the membrane and the solution ($\alpha$, $C$). For a fully retentive membrane, such that $\alpha = 0$, the wall concentration can be assumed to be equally distributed over the surface; the traditional equation of the osmotic model is then obtained:

$$J = (\Delta P - \Delta \Pi)/\mu_s R_h \quad \text{and} \quad C_p = 0$$

while for a nonretentive membrane, such that $\alpha = 1$, the concentration in the permeate is the bulk concentration $C_0$. The permeation rate is given according to Eq. (5):

$$J = \Delta P/\mu(C_0)R_h \quad \text{and} \quad C_p = C_0$$

For $0 < \alpha < 1$, the solute transfer equation can be rewritten:

$$JC_p/\Delta P = (\alpha/R_h)(C/\mu(C)) \tag{8}$$

Assuming that the two regions of different pores distribution are independent, concentration $C$ of the solution flowing through the largest pores of the membrane should be equal to that in the bulk, $C_0$. However, due to the random distribution of the pores at the membrane surface, the solutions located at the entrance of pores belonging to the two regions can mix. Hence, concentration $C$ ranges between the values of $C_0$ and $C_m$ (the concentrations in the bulk and at the membrane-solution interface). $C$ depends on the applied pressure, since the concentration at the membrane-solution interface increases when the pressure increases. Variations in the left-hand side of Eq. (8), $JC_p/\Delta P$, are plotted in Fig. 7 versus the applied pressure $\Delta P$ for various Reynolds numbers and concentrations (data from Figs. 2 and 3). On the other hand, variations in the ratio $C/\mu(C)$ obtained from viscosity measurements with the dextran T70 solution are plotted in Fig. 8. The shapes of the curves giving the variations of $JC_p/\Delta P$ versus $\Delta P$ and those of the ratio $C/\mu(C)$ versus $C$ are similar. More precisely, there is a transmembrane pressure at which the quantity $JC_p/\Delta P$ goes through a maximum, and a concentration at which the ratio $C/\mu(C)$ goes through a maximum, too, for a concentration of about 50 g/kg. Consider Eq. (4): It is possible to write an equation for the flux ratio $J_A/J$ and the concentrations ratio $C_p/C$. Because of the very low value of the concentration ratio, the flux $J_A$ can be neglected compared to

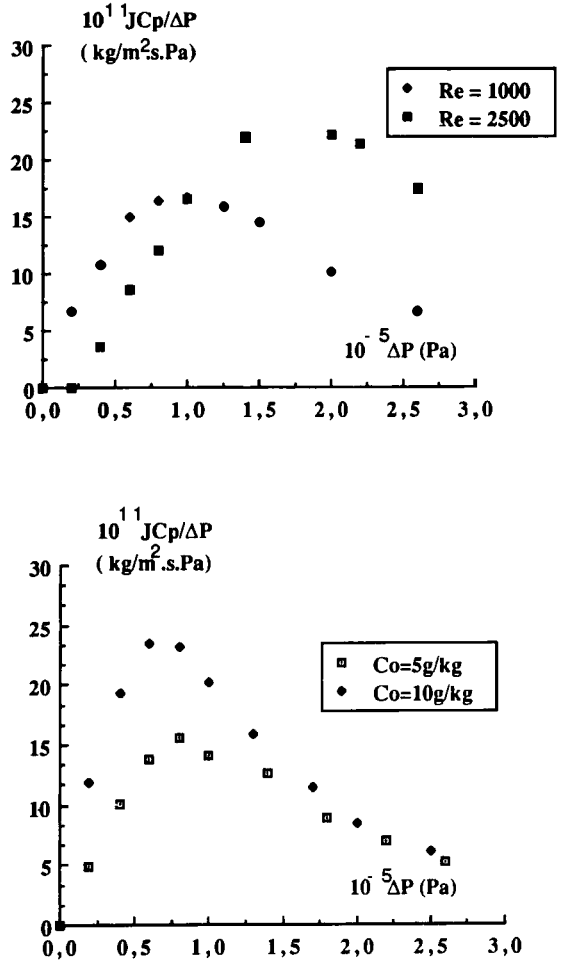


FIG. 7. Variations of the left-hand side of Eq. (8) versus applied pressure (data from Figs. 2 and 3).

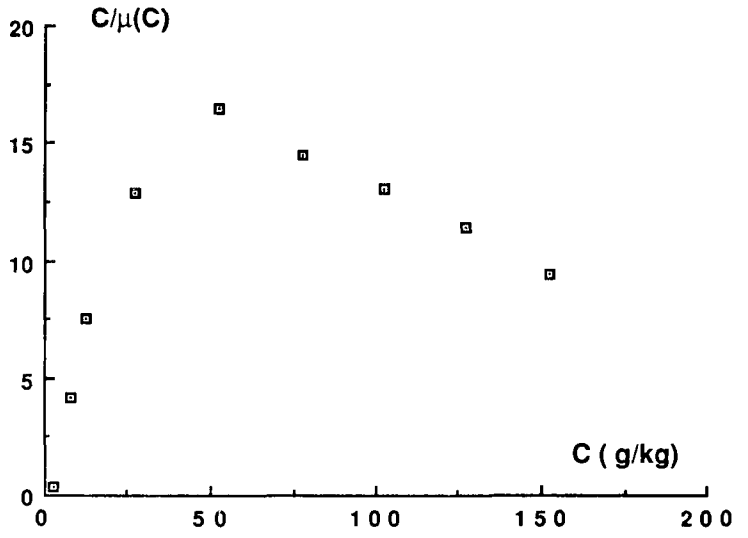


FIG. 8. Variations of the ratio $C/\mu(C)$ versus $C$ for the dextran solution (data from viscosity measurements at 20°C).



the flux $J_B$ in Eq. (3), giving the overall permeate flux $J$. As a result, the value of the concentration $C_m$ at the membrane-solution interface can be estimated by using the following equations:

$$J = (\Delta P - \Delta\Pi)/\mu(C_p)R_h \tag{9}$$

$$\Delta\Pi = \Pi(C_m) - \Pi(C_p) \tag{10}$$

In addition to these equations, it is necessary to use the relationship proposed by Ogston and Preston (*22*) for the concentration dependence of the osmotic pressure of dextran T70. In Fig. 9 the variations of $JC_p/\Delta P$, which represent the solute mass transfer according to the pore partition model, are plotted versus $C_m$. Whatever the Reynolds number and the concentration of the feed, these curves have a maximum. From a qualitative point of view, the pore partition model (Eq. 8) enables the variations of the solute transfer with the applied pressure, i.e., the concentration at the membrane interface, to be described. However, since the curves corresponding to various operating parameters are not superimposed, this suggests that the pore partition parameter varies with the operating con-

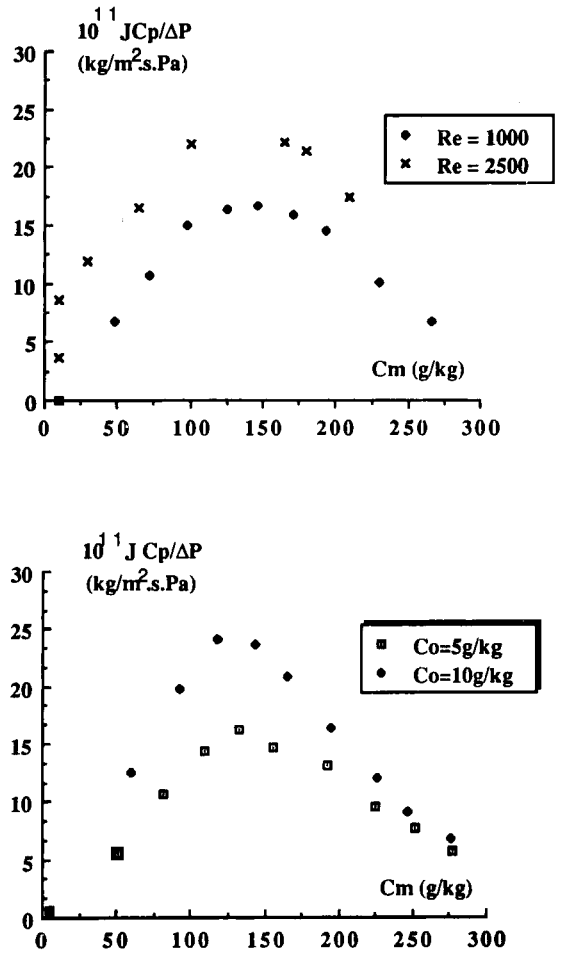


FIG. 9. Variations of the left-hand side of Eq. (8) with the concentration at the membrane-solution interface calculated from the osmotic model relationships (Eqs. 9 and 10 in the text) and from the equation proposed by Ogston and Preston (*22*) that relates osmotic pressure and concentration for dextran T70 solutions.

ditions. In the ultrafiltration of polymeric solutions, such as dextran solutions, some previous work (*14*, *16*) has shown that polymer coils can be deformed under the stress created by permeate flow through the pores as well as under the concentration increase existing near the membrane wall. As a result, when concentration polarization increases, a solute of a given molecular weight occupies less and less volume until it becomes possible for it to flow through pores of a smaller size. Consequently, the partition coefficient defined for a membrane and for a solute of a given size depends on the operating conditions affecting the concentration polarization, i.e., transmembrane pressure, feed concentration, and feed flow rate. On the other hand, gel permeation chromatography, by providing the molecular weight distributions in the feed and in the permeate, emphasizes the existence of segregation with respect to the different molecular weight solutes present in the solution (*16–18*). This should be accounted for by extending the concept of partition parameter to all sizes of molecules in a model.

This leads to a very complex model, since those partition parameters also depend on the polarization. However, in some cases it is possible to use these parameters to get information about the pore distribution of the membrane, provided that the effects of polarization have been carefully controlled (*23*).



## Particle Fouling Model

The experimental observation of the existence of a steady state during ultrafiltration of a clay suspension (Fig. 4) suggests that the flux decrease due to particles is not the consequence of a simple cake filtration mechanism that would predict a continuous decrease of flux versus time (*4*, *5*). It is therefore necessary to account for another phenomenon that balances the mass transport due to convection and leads to a steady state for mass transfer. The scour model (*6*) assumes, for example, that some particles carried to the membrane surface by the filtration of the solvent may be removed because of the tangential flow of the feed. Hence, it predicts that transfer is dependent on the operating conditions. However, such a mechanism does not explain why the presence of particles has no significant influence on the permeate flux under some conditions (Figs. 5 and 6), or how a limiting flux can be observed.

Let us now consider the membrane to be a low porosity medium whose open surface is made up of a set of pores of various sizes. A particle fouling mechanism was recently proposed by Rautenbach and Schock (*7*)

who assumed the particles and pores to be independent. According to this mechanism, a particle located in the vicinity of a pore entrance is acted on by two kinds of forces: one due to permeate flow through the pore (which tends to carry it to the pore entrance) and the other due to tangential feed flow (which tends to drag it into the bulk). It is assumed here that the relative importance of the forces determines whether or not a particle stops at a pore entrance, i.e., whether or not the particle hinders filtration of the solvent. This mechanism predicts the fouling is dependent on both the tangential velocity of the feed and the transmembrane pressure. However, it does not predict the influence of the observed feed concentration.

Since the basic idea of this model has nevertheless proven to be sensible, we suggest the following extension to improve its use. The force system applied to a particle is modified as soon as it settles over a pore and hinders filtration since the force due to filtration is now zero. Consequently, the particle will be released into the bulk due to tangential feed flow unless the suction force is strong enough to hold the particle: this is static fouling. If a particle leaves, another one can replace it, the frequency of replacement depending on the concentration of particles in the feed: this is dynamic fouling. In addition, and according to the previous section, it must be kept in mind that both particle and pore populations are spread out over a given range. A force balance must therefore be considered for each size, and consequently, different situations must be expected within a given population because of those distributions. The calculation of the forces involved is detailed in the Appendix.



Two force balances are presented. One gives the condition to be satisfied by a particle of diameter $d_p$ arriving at a pore mouth of diameter $d_{\text{pore}}$ and stopping there, and thus hindering the filtration of solvent:

$$d_{\text{pore}}^2/d_p \geq \text{constant} \cdot u/\Delta P \tag{11}$$

The other one gives the conditions to be satisfied for such a particle to be maintined at the pore entrance by the suction force:

$$(d_{\text{pore}}/d_p)^3 \geq (24\mu_s/R)(u/\Delta P) \tag{12}$$

These force balances involve operating conditions ($u$, $\Delta P$), membrane charateristics ($d_{\text{pore}}$, constant), as well as suspension properties ($d_p$) and geometry ($R$). From a general point of view, this model leads to three separate regions of pore size distribution of the membrane defined according to a given particle size, as described in Fig. 10. By increasing the pore size of a given particle, the first region contains pores that do not

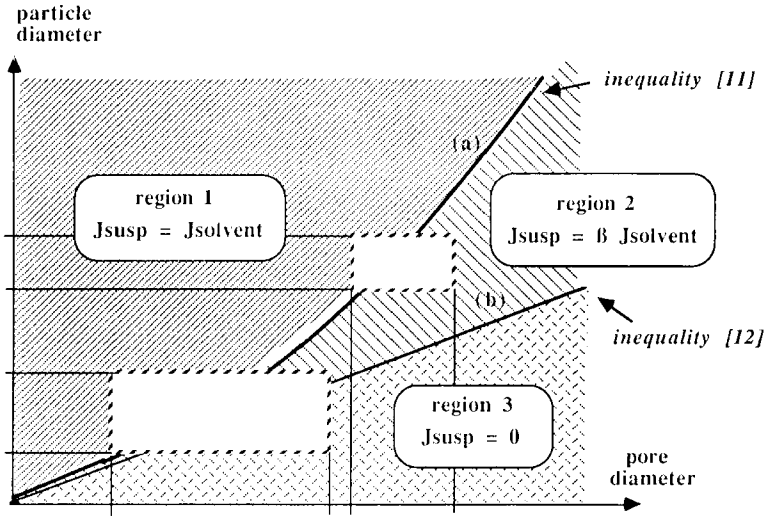


FIG. 10. Schematic representation of membrane fouling due to suspended particles.



satisfy Inequality (11). This means that a particle traveling along the surface will not stop at the pore entrance, so in this part of the membrane the flux equals that obtained for the solvent under the same conditions. The second region contains pores whose size satisfies only Inequality (11). This means that a particle arriving at the entrance of one of these pores is stopped but is not retained by the suction force. As a result, transfer through the pores in this region is hindered for a short time period, and the flux is smaller than that obtained with the solvent in the same conditions but does not equal zero. This flux depends on the concentration of particles in the feed, and that determines the fraction of time during which the pores are open to filtration of the solvent. The third region contains pores large enough for both Inequalities (11) and (12) to be satisfied. This kind of pore is plugged by static particles, and the permeate flux equals zero (this fouling is static, but reversible when the pressure is released).

Such a model predicts that the smallest particles are responsible for the more important fouling. For a given pore size distribution, the two regions in which the permeate flux is less than that of the pure solvent becomes more important as the size of the particles decreases. According to this fouling mechanism, it is possible to express the stationary values of the permeate fluxes obtained during ultrafiltration of the pure solvent and of the suspension as

$$J_{solvent} = J_1 + J_2 + J_3 \quad (13)$$

$$J_{susp} = J_1 + \beta J_2 + 0 \quad (14)$$

where $\beta$ represents the fraction of time during which the pores of Region 2 are open to the filtration of the solvent. $\beta$ depends on the concentration, and $0 < \beta < 1$. The values of $J_1$ and $J_2$ depend on such operating conditions as tangential velocity or pressure.

The influence of the operating parameters and of the membrane characteristics can be explained by using this model. For given operating conditions, increasing the pore size changes the partition of the membrane since Regions 2 and 3, through which the permeate flux is less than that obtained wih the pure solvent, become more important. Consequently, the flux decrease due to the particles becomes more important as the size of the pores increases. For a given pressure and a given concentration of particles, decreasing the feed flow rate means that the Inequalities (11) and (12) are satisfied by pores of smaller and smaller size, and this leads to a decrease in the permeate flux. The same variation is predicted for an increase of the transmembrane pressure while the feed flow rate and the concentration are kept constant. However, for pores belonging to Region 2, the fraction of time during which they are open to filtration of the solvent decreases when the concentration increases, so that the permeate flux decreases. Finally, this fouling mechanism predicts the existence of operating conditions under which neither Inequality (11) nor Inequality (12) is satisfied, so that the permeate flux obtained with the suspension equals that obtained with pure solvent under the same conditions.

A filtration problem is defined in Fig. 10 by a rectangle, the position and dimensions of which are determined by the pore size and the particle size distributions. As illustrated by the dotted lines in this figure, situations controlled by various phenomena can be expected, depending on the position of the rectangle with respect to Curves a and b. In practice, this position depends on the choice of membrane for processing a given fluid.

Since the present study uses ideal fluids, some phenomena, which in practice affect both the fluid and the membrane, have been avoided. Nevertheless, their consequences can be illustrated in a graph of the Fig. 10 type. For example, expansion of the particle size range can occur due to aggregation, particle cracking, cell rupture, etc. Such situations would be described in Fig. 10 by an enlargement of the rectangle in the direction of the vertical axis.

The other very important phenomenon to be considered in real systems is membrane fouling. It has been shown (*24*) that membrane fouling does

not affect all the pores in the same way, but depends on what kind of fouling is involved: adsorption, pore plugging, etc. For example, fouling can occur when the largest pores and the smallest particles have approximately the same size. If some particles are smaller than a pore, they can penetrate and plug it: this condition is shown in Fig. 11 by straight line (c), the slope of which is close to 1. The region under Line c represents a high risk of pore plugging. The consequence would be an irreversible reduction in the pore size range, depicted in Fig. 11 by a leftwards move of the right vertical boundary. The dynamic fouling described in the present work can then take place in the range of pores remaining open.

In filtration of suspensions, only a fraction (1) of the pores of a membrane would be ruled by Poiseuille's law, either because of permanent blocking of the largest (pore plugging (4) and static fouling (3)), or because of dynamic fouling (2) by particles acting as "bouncing" ball valves as



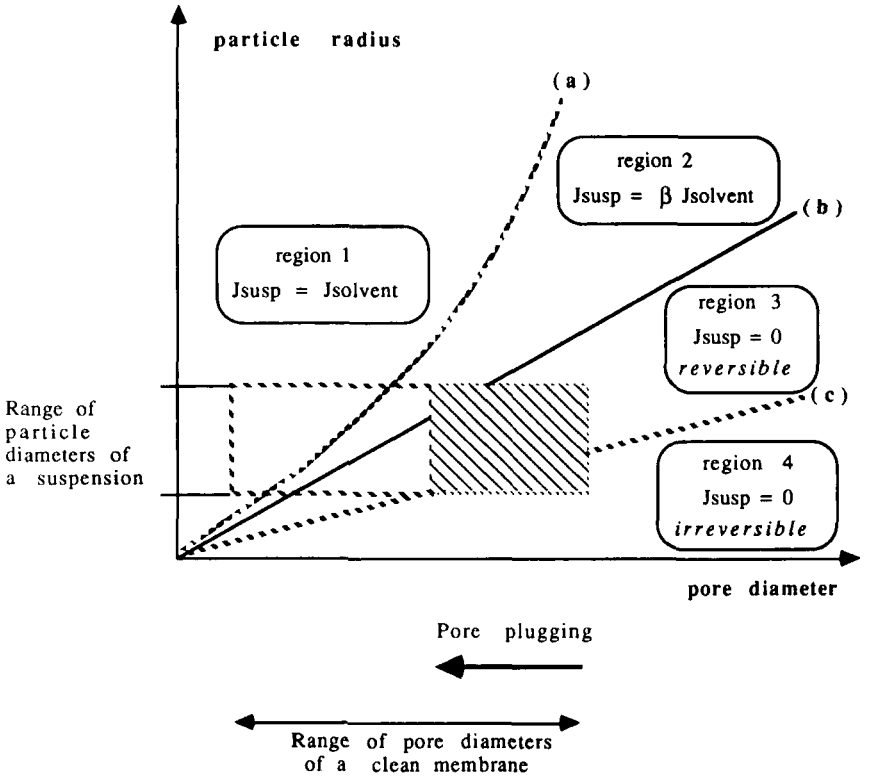


FIG. 11. Schematic representation of membrane fouling in the presence of pore plugging (c).

summarized in Fig. 12. Boundaries (a) and (b) explicitly depend on operating conditions, but that of (c) does not.

The above examples suggest that a situation can change during an experiment. The relative importance of reversible and irreversible phenomena and of dynamic and static fouling can evolve and interfere with each other due to changes in particle and pore size distribution. Therefore such operating parameters as cross flow velocity or pressure may not have the same influence at the beginning and at the end of a run.

From the point of view of solvent transfer, irreversible pore plugging and static fouling as described in this paper have the same consequence: they prevent the solvent from flowing through the pores. Within the frame of a sieving model, it is obvious that pores smaller than the smallest particles are required to avoid pore plugging. Assuming average values for the various parameters in Eq. (12) ($\mu_s = 10^{-3}$, $R = 10^{-3}$, $u = 1$, and $\Delta P = 10^5$) allows the constant to be estimated (here 0.063). According to this equation, the present model is more demanding than the sieving one, since it requires pores about sixteenfold (1/0.063) smaller than the particles (in the present example) to avoid static fouling. An estimation of the constant in Eq. (11) is difficult since two unknowns, $B_1$ and $B_2$, are used.



## CONCLUSION

Although the transfers of solvent and solute during the ultrafiltration of fluids containing either dissolved or suspended solids seem very different at first glance, it is shown here that a similar approach can be used for their description. Its main peculiarity lies in its use of classical models to account for a partition of the membrane as well as for the size distribution of the fluid components, but the improvement of existing models is also required.

In the ultrafiltration of macromolecular dextran solutions, the solute mass transfer is difficult to model due to the multiplicity and variability of the parameters involved. However, from a qualitative point of view it is possible to describe the transport of that kind of solute through ultrafiltration membranes by using an improvement of the pore partition model. That extension consists in accounting for the variability of the partition parameters according to polarization conditions because of the ability of the solutes to be deformed under the stress created by the flow at the pore entrance as well as under the concentration increase at the membrane-solution interface. The variations in solute transfer can thus be qualitatively described.

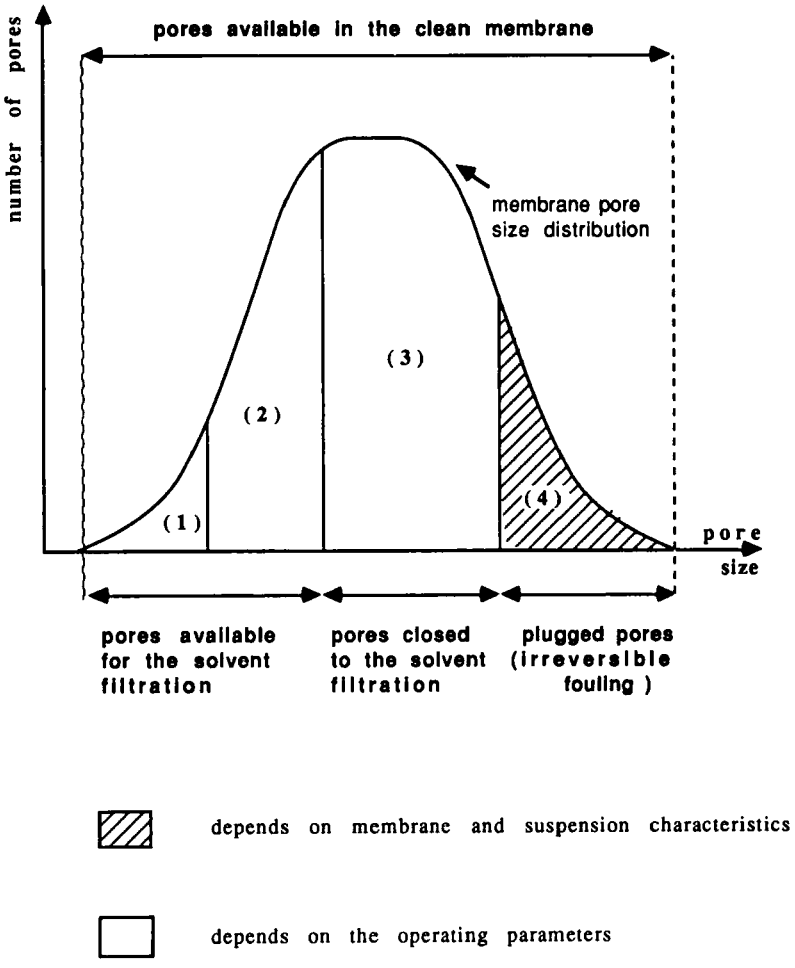


FIG. 12. Sketch showing how a pore size distribution would be affected by various mechanisms, with the dependence on the operating parameters and on the membrane.

In the ultrafiltration of clay suspensions, a fouling mechanism derived from an analysis of the various forces exerted on a particle is proposed. It is emphasized that when a particle settles at a pore mouth and hinders filtration, the drag force due to filtration is replaced by a suction force. When membrane partition as well as particle size distribution are accounted for, the conclusion is that fouling is due to plugging, dynamic or static, of the largest pores of the membrane by the smallest particles contained in the suspension. From the balance of the forces, the influence of the operating conditions and of the membrane properties on the permeate flux can be explained, as it was experimentally observed. Furthermore, it is shown how two mechanisms (pore plugging and static fouling) can have the same macroscopic consequences (i.e., no more flux through the pore) despite the fact that the effects of operating parameters are not the same on those two different mechanisms.

The present conclusions suggest that these models can be used to investigate how the presence of suspended particles influences the ultrafiltration of solutions.



## APPENDIX: FORCE BALANCE USED IN THE PARTICLE FOULING MODEL

Generally, the force $F$ exerted on a particle of diameter $d_p$ by a fluid flowing with a velocity $v$ is given by

$$F = f(\rho v^2)/2 \cdot \pi d_p^2/4 \tag{A1}$$

For laminar flow the friction coefficient $f$ is related to the Reynolds number defined according to the particle diameter:

$$f = 24/\mathrm{Re} = (24\mu)/(d_p v \rho) \tag{A2}$$

By combining these two equations:

$$F = 3\mu\pi d_p v \tag{A3}$$

## Calculation of the Forces Exerted on a Particle Carried by the Feed Flow

### *Calculation of the Tangential Force*

In laminar flow, assuming that the permeation is so low that no change is induced on the parabolic velocity profile inside the fibers, the equations giving the tangential velocity and the shear stress at a given distance, $r$, from the center of the fiber are

$$v_z(r)/v_{max} = 1 - (r/R)^2 \tag{A4}$$

$$\tau_{rz} = -\mu \partial v/\partial z = (\Delta P r)/(2L)$$

where $v_{max}$, $R$, $L$, and $\mu$ represent the velocity at the center of the fiber, the radius and the length of the fiber, and the viscosity of the flowing fluid.

Assuming that at the membrane wall the tangential velocity equals zero, and defining a new coordinate $r^* = R - r$ gives

$$v_z(r^*) = (\Delta P R)/(2\mu L) \cdot r^* \tag{A5}$$

Substituting for the pressure drop given by Poiseuille's law ($u_{average}\pi R^2 = (\Delta P \pi R^4)/(8\mu L)$) gives a relationship between the velocity at a given distance $r^*$, the average velocity $u$, and the fiber radius:

$$v_z(r^*) = (4u/R)r^* \tag{A6}$$

The tangential force $F_t$ exerted on a particle by the tangential flowing fluid then becomes

$$F_t = 12\mu u \pi d_p r^*/R \tag{A7}$$

For a particle located in the vicinity of the membrane wall, $r^* = r_p$, so that

$$F_t = 6\mu\pi u d_p^2/R \tag{A8}$$

### *Calculation of the Force Due to Convection*

To get an expression for that force requires the particle velocity in the direction normal to the membrane surface to be known. It depends on the filtration rate $v_{pore}$ through the pore. According to Poiseuille's law $v_{pore}$ is

$$v_{pore} = (\Delta P/32\mu e)d_{pore}^2 \tag{A9}$$

where $e$ is the thickness of the dense skin layer of the membrane.

Since there is no relationship between the permeation rate through a pore and the induced velocity of a particle in the vicinity of the pore entrance $v_f$, to the knowledge of the authors, the following expression is used:

$$v_f = B_1 v_{pore} \tag{A10}$$

Combined with Eq. (A3) this leads to

$$F_f = \Delta P/(32\mu e) \cdot d_{pore}^2 B_1 \tag{A11}$$

### *Forces Balance*

The forces balance to be satisfied for a particle to stop at the entrance of a pore to hinder the filtration of the solvent can be expressed by

$$F_f \geq B_2 F_t \tag{A12}$$

Substituting for $F_t$ and $F_f$ (Eqs. A8 and A11) in Eq. (A12) gives

$$d_{pore}^2/d_p \geq (\mu e/64)(\mu/\Delta P) \tag{A13}$$

### Calculation of the Forces Exerted on a Particle Located at a Pore Entrance

As soon as a particle stops at the entrance of a pore and thereby hinders the filtration of the solvent, i.e., as soon as Inequality (A13) is satisfied, it is influenced by a new system of forces in which the force $F_f$ due to permea-

tion is replaced by a static force, $F_s$, induced by the pressure gradient between the two sides of the membrane. As a result, the new forces system is

$$F_t = 6\mu\pi u d_p^2/R$$

$$F_s = (\pi d_{\text{pore}}^2/4)\Delta P \tag{A14}$$

For the particle to remain at the pore entrance, the following condition has to be satisfied

$$F_t/F_s < d_{\text{pore}}/d_p \tag{A15}$$

Substituting for $F_t$ and $F_s$ in Eq. (A15) gives

$$(d_{\text{pore}}/d_p)^3 \geq (24\mu/R)(u/\Delta P) \tag{A16}$$

If Inequality (A16) is not satisfied, the static force is not sufficient for the particle to remain at the pore entrance, and it may be removed by the tangential feed flow. Consequently, the situation is again the same as before the arrival of the particle, and another particle of the same size or smaller can replace it.



## NOMENCLATURE

| | |
|---|---|
| $C_0$ | bulk concentration |
| $C_p$ | permeate concentration |
| $d_p$ | particle average diameter |
| $d_{\text{pore}}$ | pore diameter |
| $\Delta P$ | pressure difference across the membrane |
| $e$ | pore length |
| $F_f$ | drag force due to convection through the pores |
| $F_t$ | drag force due to tangential flow |
| $F_s$ | suction force |
| $J$ | overall filtration flux |
| $J_1$ | filtration flux through nonselective pores |
| $L_p$ | membrane permeability |
| $R$ | hydrodynamic radius |
| $T.R.$ | rejection coefficient |
| $u$ | axial velocity |

## Greek

| | |
|---|---|
| $\alpha$ | fraction of pores allowing solute transport |
| $\beta$ | probability for a pore to be dynamically blocked |
| $\mu$ | viscosity |
| $\pi$ | osmotic pressure |
| $\rho$ | density |

## Acknowledgment

This work received financial support from the "Lyonnaise des Eaux" (France).



## REFERENCES

1. J. G. Wijmans, S. Nakao, and C. A. Smolders, "Flux Limitation in Ultrafiltration: Osmotic Pressure and Gel Layer Model," *J. Membr. Sci., 20,* 115 (1984).
2. R. L. Goldsmith, "Macromolecular Ultrafiltration with Microporous Membranes," *Ind. Eng. Chem., Fundam., 10,* 113 (1971).
3. A. G. Fane, "Ultrafiltration of Suspensions," *J. Membr. Sci., 20,* 249 (1984).
4. K. Schneider and W. Klein, "The Concentration of Suspensions by Means of Cross-Flow Microfiltration," *Desalination, 41,* 263 (1982).
5. T. B. Choe, P. Masse, A. Verdier, and M. J. Clifton, "Flux Decline in Batch Ultrafiltration—Concentration Polarization and Cake Formation," *J. Membr. Sci., 26,* 1 (1986).
6. A. G. Fane, C. J. D. Fell, and M. T. Nor, "Ultrafiltration in the Presence of Suspended Matter," *I. Chem. Jubilee Symp., 73,* C1 (1982).
7. R. Rautenbach and G. Schock, "Ultrafiltration of Macromolecualar Solutions and Crossflow Microfiltration of Colloidal Suspensions—A Contribution to Permeate Flux Calculation," *5th International Symposium on Synthetic Membranes in Science and Industry,* Tübingen, FRG, 1986.
8. L. J. Zeman, "Adsorption Effects in Rejection of Macromolecules by Ultrafiltration Membranes," *J. Membr. Sci., 15,* 213 (1983).
9. S. Nakao, S. Yumoto, and S. Kimura, "Analysis of Rejection Characteristics of Gel Layer for Low Molecular Weight Solutes," *J. Chem. Eng. Jpn., 6,* 463 (1982).
10. G. Capannelli, F. Vigo, and S. Munari, "Ultrafiltration Membranes—Characterization Methods," *J. Membr. Sci., 15,* 289 (1983).
11. C. Taddei, P. Aimar, G. Daufin, and V. Sanchez, "Etude du transfert de matière lors de l'ultrafiltration de lactosérum doux sur membrane minérale," *Lait, 66,* 371 (1986).
12. B. D. Mitchell and W. N. Deen, "Effect of Concentration on the Rejection Coefficients of Rigid Macromolecules in Track-Etched Membranes," *J. Colloid Interface Sci., 113,* 32 (1986).
13. A. Bottino, G. Capannelli, A. Imperato, and S. Munari, "Ultrafiltration of Hydrosoluble Polymers—Effect of Operating Conditions on the Performance of a Membrane," *J. Membr. Sci., 21,* 247 (1984).

14. G. T. Nguyen and J. Neel, "Characterization of Ultrafiltration Membranes. Part IV. Influence of the Deformation of Macromolecular Solutes on the Transport through Ultrafiltration Membranes," *Ibid., 14,* 111 (1983).
15. G. Jonsson and P. M. Christensen, "Separation Characteristics of Ultrafiltration Membranes," *Proc. Stresa, Italy* (July 1984).
16. H. de Balmann and R. Nobrega, "The Deformation of Dextran Molecules—Causes and Consequences in Ultrafiltration," *J. Membr. Sci., 40,* 311 (1989).
17. D. L. Woerner and J. L. McCarthy, "The Effect of Manipulatable Variables on Fractionation by Ultrafiltration," *AIChE Symp. Ser., Ind., Membr., Processes,* p. 77 (1986).
18. G. Schock and A. Miquel, "Characterization of Ultrafiltration Membranes: Cutoff Distribution Measurements by GPC," *1987 International Congress on Membrane and Membrane Processes ICOM,* Japan, 1987, 6-P31.
19. O. Kedem and A. Katchalsky, *Biochim. Biophys. Acta, 27,* 229 (1958).
20. S. I. Nakao and S. Kimura, "Analysis of Solutes Rejection in Ultrafiltration," *J. Chem. Eng. Jpn., 14,* 32 (1981).
21. M. S. Le and J. A. Howell, "Alternative Model for Ultrafiltration," *Chem. Eng. Res. Des., 62,* 373 (1984).
22. A. G. Ogston and N. Preston, "Macromolecular Compression of Dextran," *Biochem. J., 183,* 1 (1979).
23. R. Nobrega, H. de Balmann, P. Aimar, and V. Sanchez, "Transfer of Dextran through Ultrafiltration Membranes: A Study of Rejection Data Analyzed by Gel Permeation Chromatography," *J. Membr. Sci., 45,* 17 (1989).
24. H. de Balmann, M. Meireles, P. Aimar, and V. Sanchez, "Study of the Fouling of UF Membranes Using Gel Permeation Chromatography," *The 3rd Chemical Congress of North America,* Toronto, Canada, June 1988.

*Recieved by editor March 30, 1989*